Mesoscale eddies in the South China Sea observed with altimeter data

Guihua Wang,[1] Jilan Su,[1] and Peter C. Chu [2]

Received 2 September 2003; accepted 20 October 2003; published 13 November 2003.

[1] A composite time series (1993–2000) of sea surface height anomaly from several satellites is used to identify eddies in the South China Sea (SCS). The eddy lifetime, radius, strength, and straight-line travel distance are estimated. Altogether 58 anticyclonic eddies and 28 cyclonic eddies are identified for this period. They are grouped into four geographical zones according to known eddy generation mechanisms, and their statistics are discussed accordingly. Our geographical classification is a useful first step in gaining an overview of their generation. *INDEX TERMS:* 4520 Oceanography: Physical: Eddies and mesoscale processes; 4556 Oceanography: Physical: Sea level variations; 9320 Information Related to Geographic Region: Asia. **Citation:** Wang, G., J. Su, and P. C. Chu, Mesoscale eddies in the South China Sea observed with altimeter data, *Geophys. Res. Lett.*, *30*(21), 2121, doi:10.1029/2003GL018532, 2003.

1. Introduction

[2] The SCS is the largest semi-enclosed marginal sea in the Northwest Pacific with several passages leading to neighboring waters (Figure 1). Its connection to the Pacific is through the Luzon Strait, east of which the Kuroshio flows northward. Another important connection is the Mindoro Strait to the Sulu Sea.

[3] The upper layer circulation over the deep basin of the SCS is driven mainly by the monsoon, with significant influence from the Kuroshio for its northern part [*Qu*, 2000; *Su*, 2003]. In the winter there is a generally cyclonic gyre over the entire deep basin of the SCS, while during the summer there is a cyclonic gyre north of about 12°N and an anticyclonic gyre south of it. Associated with these gyres are coastal jets, a southward jet along the entire western boundary in winter and, in summer, a northward jet south of about 12°N and a southward jet along the northwestern boundary. The northward jet turns offshore from the Vietnam coast near 12°N in summer, identifiable from its accompanying upwelling characteristics [e.g., *Kuo et al.*, 2000]. This area is also where a mean current crosses the SCS and exits through the Mindoro Strait [*Metzger and Hurlburt*, 2001a]. The year-round southward coastal jet in the northern SCS will be called the Dongsha Current (DC) because of its proximity to Dongsha Islands [*Su*, 2003]. Southwest of Taiwan there is a small but seemingly year-round anticyclonic gyre [*Su et al.*, 1999].

[4] Embedded in the gyres are many mesoscale eddies, observed from both hydrographic [*Chu et al.*, 1998; *Su et al.*, 1999] and altimeter data [*Shaw et al.*, 1999; *Hwang and Chen*, 2000]. Based on 5 years of altimeter data over the SCS from 1992 to 1997, significant mesoscale variability in the SCS are found only in two narrow strips north of 10°N [*Wang et al.*, 2000]. The stronger one lies along the northern/western boundary near the 2000 m isobath over the lower continental slope where the DC flows nearby. The other is a NE-SW strip about 450 km wide, extending from the Luzon Strait to the Vietnam coast. However, there are only few works on the mechanisms of their generation [*Liu and Su*, 1992; *Metzger and Hurlburt*, 2001a; *Cai et al.*, 2002]. Based on the sea surface height anomaly (SSHA) from multiple satellite dataset during 1993–2000, this study focuses on the life history statistics of eddies in the SCS.

2. Data and Eddy Identification

[5] We use a multiple altimeter dataset in 1/8° × 1/8° grids from the US Naval Research Laboratory, derived from the TOPEX/POSEIDON (T/P), ERS and Geosat Follow On (GFO), with the orbit error and tides removed, as discussed by *Jacobs et al.* [2002]. We extracted a dekad (synoptic 10-day) composites covering the period from 1/1993 to 12/2000. To avoid aliasing from residual tidal effects, we apply a simple Hanning filter with a period around and shorter than 60d [*Wang et al.*, 2000].

[6] From the processed 8-year time series of SSHA, we identify and track the evolution of mesoscale eddies in the SCS according to the following 5 criteria: (1) There exist closed SSHA contours; (2) The center of the eddy is over water deeper than 1000 m; (3) The SSHA difference between its center and its outermost contour, M, is greater than 7.5×10^{-2} m [*Roemmich and Gilson*, 2001]; (4) The eddy can be tracked forward over 3 data points (30 days) under criterion 3; (5) If the above four criteria are satisfied it may be tracked back in time provided M stays greater than 4.0×10^{-2} m. The 5th criterion is chosen because the measurement error of the SSHA is around $2 \sim 3 \times 10^{-2}$ m. Altogether, 10 eddies were back-tracked in this way, 3 for 40 days, 2 for 30 days, 3 for 20 days and 2 for 10 days.

[7] Most of the tracked eddies were over waters deeper than 2000 m. There were 5 eddies, however, that traversed briefly over waters shallower than 1000 m during their long journey. Four of them passed near the Dongsha Islands and the other one crossed over a plateau south of Taiwan. In these five particular cases we have waived the 2nd criterion.

[8] Overall, our identifications of eddy location and occurrence check well against hydrographic observation by *Chu et al.* [1998], *Su et al.* [1999], *Fang et al.* [2002], the ATLAS mooring buoys of the Tropic Atmosphere Ocean (TAO) Project, as well as our own hydrographic observation in August 2000. However, our results support

[1]Laboratory of Ocean Dynamic Processes and Satellite Oceanography, Second Institute of Oceanography, SOA, Hangzhou, Zhejiang, China.
[2]Department of Oceanography, Naval Postgraduate School, Monterey, California, USA.

0094-8276/03/2003GL018532$05.00

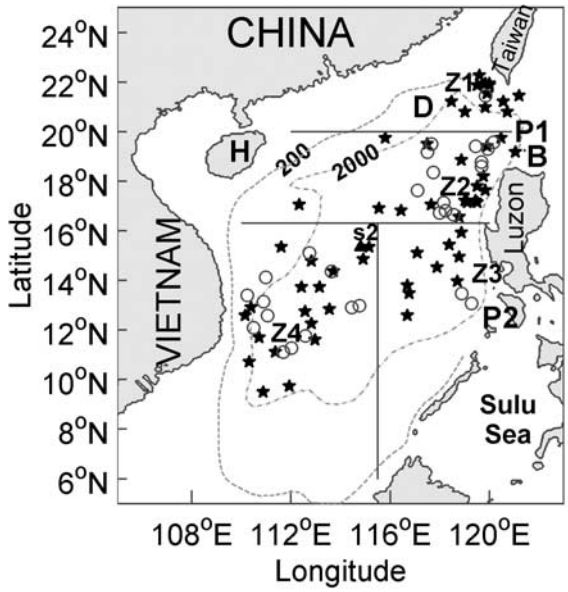

Figure 1. Map of the SCS. Isobaths are in meter. (○: cyclonic eddy; ★: anticyclonic eddy; ▲: TAO buoy S2.) B: Babuyan Islands. D: Dongsha Islands. H. Hainan Island. P1: Luzon Strait. P2: Mindoro Strait. Solid lines are boundaries for zones Z1, Z2, Z3 and Z4.

4 out of 5 eddies from the hydrographic plots for April 1998 [*Su*, 2003; Figure 6] except for the cyclonic one near (15°N, 114°E). Although their survey covered the entire SCS basin, only 3 stations were related to that particular eddy.

3. Geographical Grouping of the Eddies

[9] A total of 86 eddies generated and decayed in the SCS between 1993–2000 have been identified. To facilitate discussion of the statistics, we group them into 4 geographical zones according to where they were first formed (Figure 1). Delineation of the zones is based on the limited knowledge of the eddy generation mechanisms in the SCS. They are, respectively, Z1: Southwest of Taiwan, Z2: Northwest of Luzon, Z3: Southwest of Luzon and Z4: Offshore of Central Vietnam. The second zone actually extends all the way west to the 1000 m isobath.

[10] **Zone Z1:** With a 6-layer numerical model, *Metzger and Hurlburt* [2001a] finds that pinch-off of an anticyclonic eddy (A-eddy) can occur when the Kuroshio intrudes deeply into Z1. A subsequent work by *Metzger and Hurlburt* [2001b] showed that, when grids finer than 1/16 degree are used, deep Kuroshio intrusion into the SCS is less likely because of better representation of the small islands in the Luzon Strait. Indeed, so far synoptic observations have found the Kuroshio intrusion limited to approximately 119°E [*Su*, 2003]. Nevertheless, frontal instability at the Kuroshio intrusion could be one mechanism in shedding mesoscale eddies [*Wang et al.*, 2000; *Su*, 2003]. Such intrusion usually takes place during the winter monsoon [*Wang and Chern*, 1987].

[11] **Zone Z2:** *Metzger and Hurlburt* [2001a] also finds that generation of A-eddy can occur in August/September west of the Babuyan Islands in eastern Z2. A likely mechanism generating a cyclonic eddy (C-eddy) is the intense positive wind stress curl offshore northwest of Luzon in winter [*Qu et al.*, 2000]. A third mechanism arises from the (positive) vorticity advected westward from the Kuroshio front [*Liu and Su*, 1992]. Their reduced-gravity model shows a large basin-scale fluctuating cyclonic gyre, inside of which a C-eddy is periodically developed at its eastern end, migrates westward and eventually pinches off. In the process, an A-eddy with less strength is also induced southeast of the gyre. We note that such mechanism is likely stronger in winter when the Kuroshio intrudes into the SCS.

[12] **Zone Z3:** In northern Z3, C-eddies were found with AXBT data [*Chu et al.*, 1998] and a warm pool in the upper 300 m was identified with hydrographic data [*Su et al.*,

Table 1. Zonal Eddy Statistics

Zone		Z1		Z2		Z3		Z4	
Eddy Type		A	C	A	C	A	C	A	C
Monthly Distribution of Eddy Generation	Jan	1	0	1	2	2	0	2	0
	Feb	0	0	0	2	1	0	2	2
	March	0	1	0	2	1	1	5	1
	April	0	0	4	0	2	0	0	0
	May	1	0	4	0	0	0	3	2
	June	1	0	4	0	0	0	4	1
	July	1	0	1	1	0	0	1	1
	Aug	0	0	2	0	0	0	1	3
	Sept	2	0	0	1	0	0	0	0
	Oct	3	0	1	0	0	0	0	1
	Nov	2	0	0	1	2	0	0	0
	Dec	2	0	1	4	1	1	0	1
Total Eddies		13	1	18	13	9	2	18	12
$\langle T \rangle$		108	100	130	140	170	100	125	140
$\langle L \rangle$		195	160	414	387	477	173	210	140
$\langle V \rangle$		1.82	1.64	2.85	2.77	3.46	2.85	1.82	0.95
$\langle D_m \rangle$		244	281	307	265	296	274	340	388
$\langle M_m \rangle$		12	9	15	14	10	12	13	16
Max (M)		32	13	30	28	27	18	33	28
$\langle \Omega_m \rangle$		−18	12	−16	21	−13	15	−16	14

(A: anticyclonic; C: cyclonic; T: the lifetime of an eddy, in d; M_m: the lifetime mean of M of an eddy, in 10^{-2} m; D_m: the lifetime mean of an eddy's diameter (half of the sum of its E-W and N-S extents), in km L: the straight line distance between an eddy's initial and end positions, in km; V = L/T: a measure of eddy speed, in km d^{-1}; Ω_m: the lifetime mean of Ω of an eddy, in $10^{-6}s^{-1}$; Average, $\langle\ \rangle$, is with respect to the group).

Table 2. Percentage (%) of Occurrence of Multiple Eddies in a Dekad Between 1993–2000

Eddy number	0	1	2	3	4	5	6	7	8	9
A	1	0	7	34	32	20	6	0	0	0
C	15	0	42	21	20	2	0	0	0	0
A & C	1	0	0	8	21	28	23	11	7	1

(A: anticyclonic; C: cyclonic).

1999]. Using a coupled single-layer and two-layer hybrid model, *Cai et al.* [2002] suggested that, in winter, interaction between strong barotropic shelf currents and the local topography can generate an A-eddy over a deep trough in southern Z3. However, satellite altimetry data do not show high mesoscale variability in that area [*Wang et al.*, 2000; also Section 4].

[13] **Zone Z4:** Synoptic surveys often found eddies in Z4 [*Su et al.*, 1999; *Fang et al.*, 2002]. The strong eastward baroclinic jet around 12°N in summer (reaching from the Vietnamese coast to close to 115°E based on our SSHA results) is likely to generate eddies. So far there is no published work on eddy generation in this area, although model results did find dipole mode off Vietnam in summer [*Metzger and Hurlburt*, 2001a].

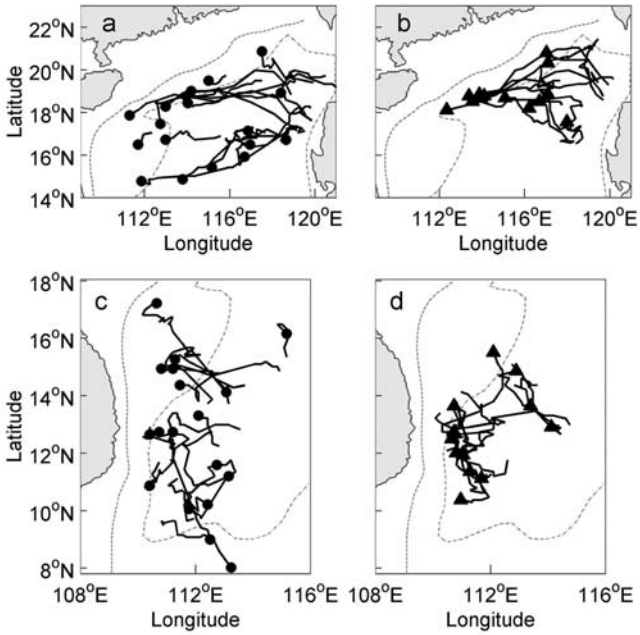

Figure 3. As in Figure 2 for Z2 (a and b) and Z4 (c and d).

4. Results and Discussion

[14] Of the 86 identified eddies with complete life history between 1993–2000, 58 and 28 are, respectively, A- and C-eddies. A typical eddy in the SCS has a lifetime about 130 days, With a mean M and radius around, 14×10^{-2} m and 300 km, respectively. C-eddies originated mainly in Z2 and Z4, and only 1 (2) was identified in Z1 (Z3), respectively (Table 1). These 3 C-eddies will not be included in the following discussion on eddy statistics. There were also more A-eddies generated in Z2 and Z4. The annual number of generation of C-eddy, A-eddy and both eddies ranges, respectively, 2 ~ 7, 6 ~ 9 and 9 ~ 14. There is a high percentage of occurrence of multiple eddies in a dekad during 1993–2000, although in 15% of the period there were no occurrence of C-eddies (Table 2).

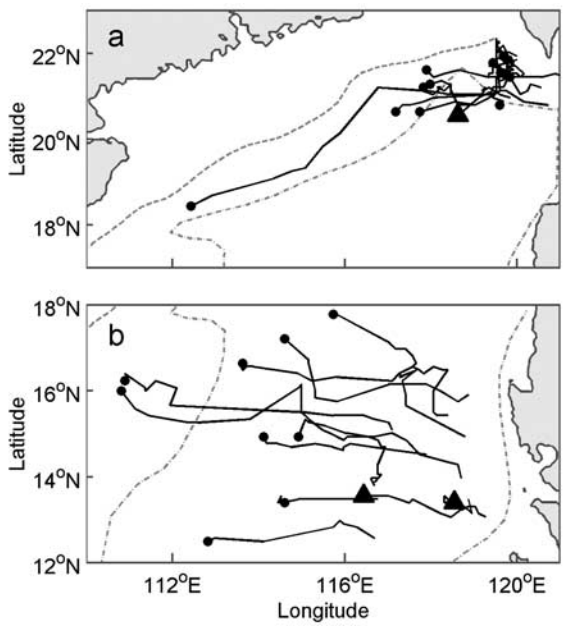

Figure 2. Tracks of A-eddies (solid line ending in solid circle) and C-eddies (solid line ending in solid triangle) generated in (a) Z1 and (b) Z3.

[15] A-eddies in Z2 and C-eddies in Z4 both have a comparatively higher average lifetime-mean M than the other groups of eddies (Table 1). We may approximate the relative vorticity (Ω) of an eddy simply by the difference between $\Delta V/\Delta X$ and $\Delta U/\Delta Y$, where ΔX (ΔY) is the latitudinal (meridional) extent of the eddy, and ΔU (ΔV) the difference between the meridional (latitudinal) velocity at both ends of ΔY (ΔX). Now we find that the A-eddies in Z1 and C-eddies in Z2 both have considerably larger magnitude in their respective average lifetime-mean Ω than those of the other groups of eddies (Table 1). This difference between the statistics of M and Ω is due to the combined effects of variations in M, D, and the Coriolis parameter (f), because, for a circular eddy, the magnitude of its Ω is equal to $8gM/fD^2$, where g is the gravitational acceleration.

[16] **Zone Z1:** 13 of the 14 eddies identified in Z1 are anticyclonic, 10 of which generated during the northeast monsoon (at least one each year), consistent with the eddy generation mechanisms discussed in Section 3. On average, compared to eddies generated in other zones, A-eddies in Z1 have small radius and short lifetime, and do not travel far. Some stayed inside the small anticyclonic gyre SW of Taiwan and others traveled to the Dongsha Island area. One A-eddy generated in 1996, however, traveled fast WSW over 800 km in distance (Figure 2a). It is the strongest and largest of the 13 A-eddies.

[17] **Zone Z2:** Most of the C-eddies in Z2 are generated during the northeast (NE) monsoon, consistent with the C-eddy generation mechanisms discussed in Section 3. The tracks of the C-eddies trace the pattern of a cyclonic gyre (Figure 3b). The average travel distance of A and C eddies in Z2 is about 400 km, rather far for eddies in the SCS.

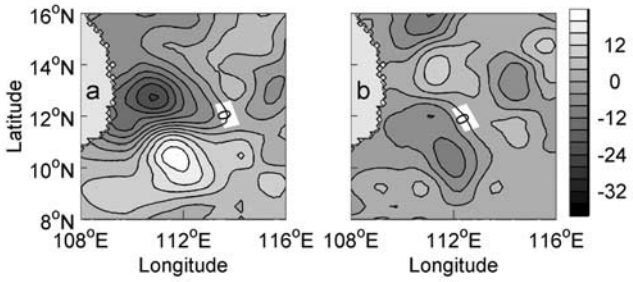

Figure 4. SSHA (10^{-2} m) distribution near Central Vietnam coast in (a) middle July 1994 and (b) 3rd dekad in Mar, 1996.

A-eddies tend to occur after the cessation of the NE monsoon and/or during the southwest (SW) monsoon. Inducement of A-eddy in the process of C-eddy generation through vorticity advection could be one mechanism. Likelihood of A-eddy generation through Kuroshio-Babuyan Islands interaction is difficult to assess because of the lack of data. The tracks of the 7 A-eddies centered initially north of 18°N also trace the pattern of a cyclonic gyre, while 9 out 11 of the A-eddies centered initially to the south traveled west or west of southwest (Figure 3a). However, uncertainty in identifying the position of an eddy center is likely to be 1/4° in latitude. We also note the generation of 4 A-eddies during the strong ENSO event between 4/1997 and 6/1998.

[18] **Zone Z3:** 9 of the 11 eddies identified in Z3 are anticyclonic, generated during or immediately after the NE monsoon. There were no eddies generated in 1995 and 2000. The only 2 C-eddies were generated in 1997 during the strong ENSO event, and, interestingly, only one A-eddy occurred in the last dekad during 1997–1998. All eddies in Z3 traveled west or west of northwest (Figure 2b). On average, compared to eddies generated in other zones, A-eddies in Z3 have long lifetime and travel far and fast.

[19] **Zone Z4:** The strong eastward jet during SW monsoon is usually accompanied by a dipole with an A-eddy (C-eddy) south (north) of the jet (Figure 4a). There is, however, equally likelihood of A-eddies generation during the NE monsoon. Two scenarios may be identified. One scenario is that, amidst the general cyclonic winter circulation background, a large anticyclonic gyre off the Vietnamese coast around 12 $\sim$ 14°N is either present throughout the winter or evolves gradually. From this gyre an A-eddy emerges. The other scenario is that an A-eddy appears to grow from a disturbance from the east. As discussed above in [11] there are two possible mechanisms generating A-eddies. In fact, numerical results of *Metzger and Hurlburt* [2001a] show that the A-eddy arising from Kuroshio-Babuyan Islands interaction in summer can sometimes reach Vietnam in winter. For either scenario the end result is a different type of dipole with an A-eddy north of a C-eddy (Figure 4b). Compared to the A-eddies in summer, the winter ones are much weaker.

[20] Mesoscale eddies are a constant feature in the SCS. Our geographical classification is a useful first step in gaining an overview of their generation, but not their dynamics. Likely mechanisms include the Kuroshio intrusion SW of Taiwan, vorticity advection from the Kuroshio, Kuroshio-Island interaction, the eastward baroclinic jet off Vietnam and the intense wind-stress curl northwest off Luzon. Other eddy generation mechanisms remain to be identified.

[21] **Acknowledgments.** This study, as a partial for fulfillment for WGH's Ph.D. requirement at Ocean University of China, was supported by the Major State Basic Research Program (G1999043805). We thank the Naval Research Laboratory, USA for providing the SSHA dataset and the Tropic Atmosphere Ocean Project for providing the ATLAS mooring data.

References

Cai, S. Q., J. L. Su, Z. J. Gan, and Q. Y. Liu, The numerical study of the South China Sea upper circulation characteristics and its dynamic mechanism in winter, *Cont. Shelf Res.*, *22*, 2247–2264, 2002.

Chu, P. C., C. W. Fan, C. J. Lozano, and J. L. Kerling, An airborne expendable bathythermograph survey of the South China Sea, May 1995, *J. Geophys. Res.*, *103*, 21,637–21,652, 1998.

Fang, W. D., G. H. Fang, P. Shi, Q. Z. Haung, and Q. Xie, Seasonal structures of upper layer circulation in the southern South China Sea from in situ observations, *J. Geophys. Res.*, *C11*(3202), doi:10.1029/2002JC001343, 2002.

Hwang and Chen, Circulations and eddies over the South China Sea derived from TOPEX/Poseidon altimetry, *J. Phys. Oceanogr.*, *105*(10), 23,943–23,965, 2000.

Jacobs, G. A., C. N. Barron, D. N. Fox, K. R. Whitmer, S. Klingenberger, D. May, and J. P. Blaha, Operational Altimeter Sea Level Products, *Oceanography*, *15*(1), 13–21, 2002.

Kuo, N. J., Q. A. Zheng, and C. R. Ho, Satellite Observation of Upwelling along the Western Coast of the South China Sea, *Remote Sens. Environ.*, *74*, 463–470, 2000.

Liu, X. B., and J. L. Su, A reduced gravity model of the circulation in the South China Sea, *Oceanologia et Limnologia Sinica*, *23*, 167–174, (in Chinese), 1992.

Metzger, E. J., and H. Hurlburt, The nondeterministic nature of Kuroshio penetration and eddy shedding in the South China Sea, *J. Phys. Oceanogr.*, *31*, 1712–1732, 2001a.

Metzger, E. J., and H. Hurlburt, The importance of high horizontal resolution and accurate coastline geometry in modeling South China Sea inflow, *Geophys. Res. Lett.*, *28*, 1059–1062, 2001b.

Qu, T. D., Upper-layer circulation in the South China Sea, *J. Phys. Oceanogr.*, *30*, 1450–1460, 2000.

Qu, T. D., T. Mitsudera, and T. Yamagata, Intrusion of the North Pacific waters into the South China Sea, *J. Geophys. Res.*, *105*(C3), 6415–6424, 2000.

Roemmich, D., and J. Gilson, Eddy transport of Heat and Thermocline Waters in the North Pacific: A Key to Interannual/Decadal Climate Variability, *J. Phys. Oceanogr.*, *31*, 675–687, 2001.

Shaw, P. T., S. Y. Chao, and L. Fu, Sea surface height variations in the South China Sea from satellite altimetery, *Oceanol. Acta*, *22*(1), 1–17, 1999.

Su, J. L., Overview of the South China Sea Circulation and its Influence on the Coastal Physical Oceanography near the Pearl River Estuary, *Cont. Shelf Res.*, in press, 2003.

Su, J. L., J. P. Xu, S. Q. Cai, and O. Wang, Gyres and eddies in the South China Sea, Onset and Evolution of the South China Sea Monsoon and Its Interaction with the Ocean, edited by Ding Yihui and Li Chongyin, China Meteorological Press, 272–279, 1999.

Wang, J., and C. S. Chern, The warm-core eddy in the northern South China Sea, I, Preliminary observations on the warm-core eddy, *Acta Oceanographica Taiwanica*, *18*, 92–103, (in Chinese), 1987.

Wang, L. P., C. J. Koblinsky, and S. Howden, Mesoscale variability in the South China Sea from the TOPEX/Poseidon altimetry data, *Deep Sea Res., Part I*, *47*, 681–708, 2000.

P. C. Chu, Department of Oceanography, Naval Postgraduate School, Monterey, CA, USA.

G. Wang and J. Su, Laboratory of Ocean Dynamic Processes and Satellite Oceanography, Second Institute of Oceanography, SOA, Hangzhou, Zhejiang, China. (guihua_wanggh@yahoo.com.cn)